Title
Constraints on the Obliquities of Kepler Planet-hosting Stars

Journal
The Astronomical Journal, 154(6)

ISSN
0004-6256

Authors
Winn, Joshua N
Petigura, Erik A
Morton, Timothy D
et al.

Publication Date
2017-12-01

DOI
10.3847/1538-3881/aa93e3

DRAFT VERSION NOVEMBER 27, 2017
Preprint typeset using LaTeX style AASTeX6 v. 1.0

CONSTRAINTS ON THE OBLIQUITIES OF *KEPLER* PLANET-HOSTING STARS

JOSHUA N. WINN[1], ERIK A. PETIGURA[2,8], TIMOTHY D. MORTON[1], LAUREN M. WEISS[3,9], FEI DAI[4,1], KEVIN C. SCHLAUFMAN[5], ANDREW W. HOWARD[2], HOWARD ISAACSON[6], GEOFFREY W. MARCY[6,10], ANDERS BO JUSTESEN[7], AND SIMON ALBRECHT[7]

[1]Princeton University, Princeton, NJ 08540, USA
[2]California Institute of Technology, Pasadena, CA 91125, USA
[3]Institut de Recherche sur les Exoplanètes, and Université de Montréal, Montréal, Canada
[4]Massachusetts Institute of Technology, Cambridge, MA 02139, USA
[5]Johns Hopkins University, Baltimore, MD 21218, USA
[6]University of California at Berkeley, Berkeley, CA 94720, USA
[7]Stellar Astrophysics Centre, Department of Physics and Astronomy, Aarhus University, Ny Munkegade 120, DK-8000 Aarhus C, Denmark
[8]Hubble Fellow
[9]Trottier Fellow
[10]Professor Emeritus

ABSTRACT

Stars with hot Jupiters have obliquities ranging from 0° to 180°, but relatively little is known about the obliquities of stars with smaller planets. Using data from the California-*Kepler* Survey, we investigate the obliquities of stars with planets spanning a wide range of sizes, most of which are smaller than Neptune. First, we identify 156 planet hosts for which measurements of the projected rotation velocity ($v \sin i$) and rotation period are both available. By combining estimates of v and $v \sin i$, we find nearly all the stars to be compatible with high inclination, and hence, low obliquity ($\lesssim$20°). Second, we focus on a sample of 159 hot stars ($T_{\rm eff} > 6000$ K) for which $v \sin i$ is available but not necessarily the rotation period. We find six stars for which $v \sin i$ is anomalously low, an indicator of high obliquity. Half of these have hot Jupiters, even though only 3% of the stars that were searched have hot Jupiters. We also compare the $v \sin i$ distribution of the hot stars with planets to that of 83 control stars selected without prior knowledge of planets. The mean $v \sin i$ of the control stars is lower than that of the planet hosts by a factor of approximately $\pi/4$, as one would expect if the planet hosts have low obliquities. All these findings suggest that the *Kepler* planet-hosting stars generally have low obliquities, with the exception of hot stars with hot Jupiters.

Keywords: stars: rotation — planets and satellites — planet-star interactions

1. INTRODUCTION

One might expect good alignment between the rotation of a star and the revolutions of its planets, and indeed, the Sun has a low obliquity. Nevertheless, some exoplanetary systems have spin-orbit misalignments, for reasons that remain unknown [see, e.g., Triaud et al. (2010); Albrecht et al. (2012), or the review by Winn & Fabrycky (2015)]. Among the proposed reasons are a primordial tilt of the protoplanetary disk (Batygin 2012), gravitational interactions between planets (Chatterjee et al. 2008), Kozai-Lidov oscillations of a planetary orbit (Fabrycky & Tremaine 2007), spin-orbit interactions between the star and short-period planets (Spalding & Batygin 2014), and angular momentum redistribution within the star (Rogers et al. 2012). In short, our ignorance is such that we do not know whether to blame the disk, the planets, the star, or a neighboring star.

Most of our knowledge of obliquities is limited to stars with close-in giant planets, with sizes $\gtrsim 6\ R_\oplus$ and orbital periods $\lesssim 10$ days. This is for practical reasons. Several of the techniques for determining obliquities rely on transit signals, which are easier to detect for close-in giant planets. Relatively little is known about stars with smaller planets or wider-orbiting planets. This is a major gap in our understanding because the *Kepler* mission has revealed that close-in giant planets are rare in comparison to systems of smaller and wider-orbiting planets (Howard et al. 2012). The *Kepler* sample of planetary systems is dominated by planets smaller than 4 $R_\oplus$ with periods ranging from 3 to 100 days.

Stellar obliquities have been measured in only a few of the *Kepler* planetary systems (Hirano et al. 2012b; Sanchis-Ojeda et al. 2012, 2013; Chaplin et al. 2013; Huber et al. 2013; Campante et al. 2016). Based on an analysis of five *Kepler* stars with multiple transiting planets, all of which were found to have low obliquities, Albrecht et al. (2013) suggested that the high obliquities are confined to hot-Jupiter hosts. Soon afterward, Huber et al. (2013) found a high obliquity for Kepler-56 (Huber et al. 2013), which remains the only system known to have two or more coplanar planets and a misaligned star. In that case, the misalignment may have been caused by the torque from a wider-orbiting third planet (Otor et al. 2016; Gratia & Fabrycky 2017).

Mazeh et al. (2015) made an important advance by mea-

suring the amplitude of photometric variability associated with rotation for a large sample of *Kepler* stars. Among the stars with effective temperatures $\lesssim 6000$ K, those without detected transiting planets displayed a lower level of variability than stars with detected planets. The ratio was approximately $\pi/4$, as one would expect if the planet-hosting stars have low obliquities and the others are randomly oriented. For hotter stars (6000-6500 K) the variability enhancement of transit hosts was not seen, suggesting that hot stars have more random obliquities. These results seemed to harmonize with previous studies of hot-Jupiter hosts, which showed that hot stars have a broader obliquity distribution than cool stars (Schlaufman 2010; Winn et al. 2010a; Albrecht et al. 2012). Thus, the variability study suggested that hot stars have a broad range of obliquities regardless of the properties of their planets, a potentially important clue to the origin of spin-orbit misalignments. The boundary of $\approx$6000 K[1] may be related to the "Kraft break" that distinguishes cool stars with thick convective envelopes from hot stars with radiative envelopes (Struve 1930; Schatzman 1962; Kraft 1967).

In this paper we report on further explorations of the obliquities of *Kepler* stars, enabled by the California-*Kepler* Survey [CKS: Petigura et al. (2017); Johnson et al. (2017)]. The CKS team performed high-resolution optical spectroscopy of about a thousand stars with transiting planets, provided a homogeneous catalog of spectroscopic parameters, and clarified the masses and sizes of the stars and their planets. Of greatest importance for our work are the measurements of the projected rotation velocity, $v \sin i$, for which the CKS team demonstrated an accuracy of $\approx$1 km s^{-1} (Petigura 2015). We used these data in three different ways:

1. For stars with reliable determinations of $v \sin i$, stellar rotation period $P_{\rm rot}$, and stellar radius $R_\star$, it is possible to derive a constraint on the stellar inclination by comparing $v \sin i$ and $v \equiv 2\pi R_\star / P_{\rm rot}$. This method has been employed by Walkowicz & Basri (2013), Hirano et al. (2012a), Hirano et al. (2014) and Morton & Winn (2014), among others. The latter authors found 2σ evidence that stars with multiple transiting planets ("multis") have lower obliquities than stars with only one detected transiting planets ("singles"). The CKS provides a larger, more accurate and more homogeneous dataset than was previously available.

2. High-obliquity systems can sometimes be recognized by virtue of an anomalously low $v \sin i$ for a star of a given type. This is because the orbital inclination $i_{\rm o}$ must be near 90° for transits to occur, and a low obliquity for a transiting-planet host implies $\sin i \approx \sin i_{\rm o} \approx 1$. Schlaufman (2010) devised a statistic to quantify the meaning of "anomalously low" and computed it for a large sample of hot-Jupiter systems. With the CKS data, we can apply this and related techniques to a larger and more diverse sample of planetary systems.

3. We can also test for systematically low obliquities by comparing the $v \sin i$ distribution of transiting-planet hosts with that of a sample of randomly oriented stars. Low-obliquity planet hosts must have $\sin i \approx 1$, whereas randomly oriented stars have $\langle \sin i \rangle = \pi/4$. Thus, if the planet hosts have low obliquities, the mean $v \sin i$ of the randomly oriented stars should be lower than that of the planet hosts by a factor of $\pi/4$.

We used these techniques to search for individual systems with high obliquities, and to perform statistical comparisons between different populations of planet-hosting stars. We compared multis and singles, stars with different types of planets, and hot vs. cool stars. We also tried to test the notion that hot stars have nearly random obliquities regardless of the properties of their planets, as suggested by the prior study of variability amplitudes.

These methods have some limitations that are common to any $\sin i$-based technique. First, they are unable to distinguish between prograde and retrograde motion. Second, because of the flattening of the sine function near 90°, it is difficult to distinguish between inclinations in the range 45°–90°. Third, even if the inclination is found to be near 90°, the stellar obliquity is not necessarily small. This is because the inclination is only one aspect of the obliquity θ:

$$\cos\theta = \sin i \, \cos\lambda \, \sin i_{\rm o} + \cos i \, \cos i_{\rm o} \approx \sin i \, \cos\lambda, \qquad (1)$$

where λ is the sky-projected angle between the rotational and orbital axes. Another useful relation between θ and i is

$$\cos i = \sin\theta \cos\phi, \qquad (2)$$

where ϕ is the azimuthal angle of the line of sight projected onto the star's equatorial plane. It is safe to assume that ϕ is uniformly distributed in a sample of unrelated stars. This is what gives $\sin i$-based techniques the power to infer the obliquity distribution of a population of stars.

This paper is organized as follows. Section 2 presents the data and the properties of the stars and planets in our sample. Section 3 considers the stars with measured rotation periods, and compares estimates of the true and projected rotation velocities. Section 4 presents two tests for anomalously low values of $v \sin i$. Section 5 compares the $v \sin i$ distributions of different samples of planet-hosting stars with one another and with a sample of stars selected without prior knowledge of any planets. Section 6 summarizes the results and their relationship to the questions raised in this introduction, and makes suggestions for future work.

2. DATA

Petigura et al. (2017) presented spectroscopic parameters for 1305 stars designated as *Kepler* Objects of Interest (KOIs). These stars have two things in common: they were selected as targets for the *Kepler* mission according to the criteria of Batalha et al. (2010), and at least one photometric signal was detected that resembles the expected signal of a transiting planet. The spectroscopic parameters were derived using `SpecMatch` (Petigura 2015). This code fits

[1] The temperature separating the different obliquity regimes was observed to be about 6250 K by Winn et al. (2010a) and found to be 6090^{+150}_{-110} K in a statistical analysis by Dawson (2014).

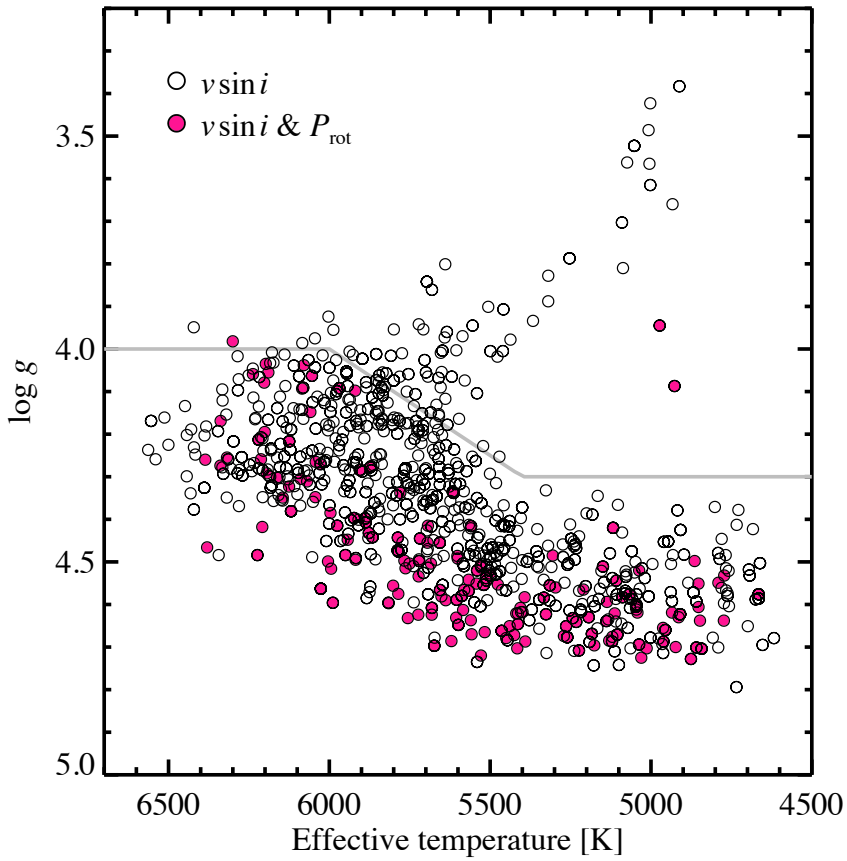

Figure 1. The stars. Spectroscopic parameters are from Petigura et al. (2017). The colored points are those for which a reliable measurement of the rotation period is available. The stars below the gray line are those we consider "dwarfs."

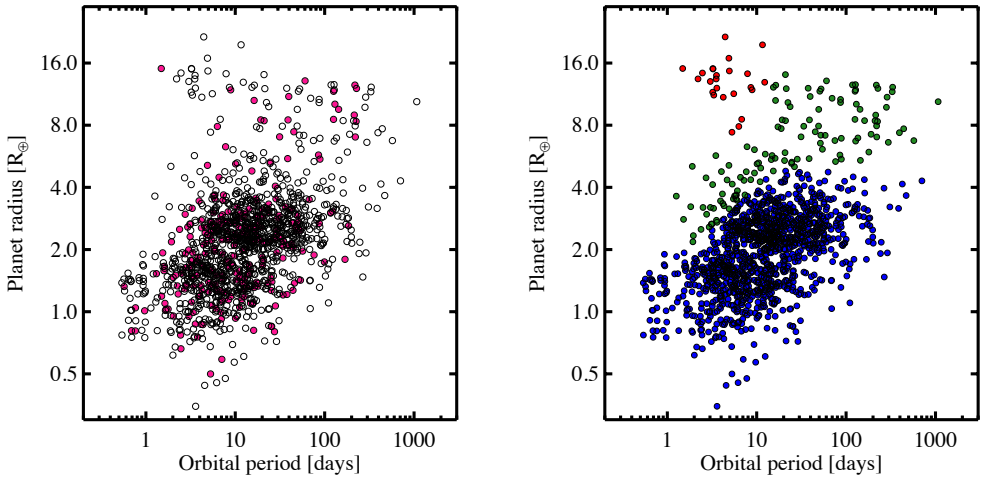

Figure 2. The planets. *Left.*—Colored points are those for which a reliable measurement of the rotation period is available, as in Figure 1. *Right.*—Same, but color-coded according to our chosen planet categories (see the text).

selected regions of an observed spectrum with a synthetic spectrum. The synthetic spectrum is generated by interpolating between theoretical spectra in the library of Coelho et al. (2005) and convolving with broadening kernels for rotation, macroturbulence, and instrumental resolution. Macroturbulence is assumed to depend on effective temperature, according to Equation (1) of Valenti & Fischer (2005).

For our study, we selected the 768 stars with planets designated as "confirmed" by Petigura et al. (2017), who based their assessment on work by Morton et al. (2016) and Mullally et al. (2016). We omitted three stars (KOI 935, 1060, and 1102) for which the $v \sin i$ measurement was found to be unreliable, after testing for internal consistency between the fits to different regions of the spectrum. This left a sample of 765 stars.

Petigura (2015) gauged the accuracy of the CKS projected rotation velocities through comparisons to measurements based on the Rossiter-McLaughlin effect (Albrecht et al. 2012). For stars with $v \sin i > 2$ km s^{-1}, he found the accuracy to be 1 km s^{-1} or better. For lower projected rotation velocities he found that the results provide only an upper limit. As a convenient interpolation between these cases, we adopted uncertainties (in km s^{-1}) of

$$1 + \frac{1}{(v \sin i/2)^4 + 1}. \quad (3)$$

To assign rotation periods to CKS stars we consulted the catalogs of Mazeh et al. (2015) and Angus et al. (2017).[2] These groups used two different techniques to detect quasiperiodic photometric variations associated with the rotation of starspots or other inhomogeneities on the stellar surface. We considered a period to be reliable if it appears in both catalogs with the same value to within 10%. There are 232 stars in our sample with a photometric period in the catalog of Mazeh et al. (2015), of which 179 are also in the catalog of Angus et al. (2017) with a matching period. From this sample we omitted 23 stars for which Furlan et al. (2017) found the *Kepler* photometric aperture to contain a stellar companion with a brightness within 3 mag of that of the intended target star. In such cases, it is not clear which star is producing the photometric variations. This left a sample of 156 stars with reliably measured photometric periods. We examined all the light curves and confirmed visually that the tabulated periods are reasonable.

Figure 1 shows the effective temperature and surface gravity of all 765 stars, and identifies the 156 stars (20% of the total) with reliably measured photometric periods. The stars with periods have systematically higher surface gravity, an indication of smaller size and younger age. This is consistent with the well-known tendency of young stars to be more active and spotted than older stars. The stars below the gray line are those we consider "dwarfs" in the sections to follow. It is defined by two horizontal lines at $\log g = 4.0$ and 4.3, joined by a straight line between $T_{\rm eff} = 5400$ K and 6000 K.

[2] The published work of Angus et al. (2017) does not include a table of rotation periods. T. Morton furnished a list of periods from that study that are deemed reliable based on inject-and-recover simulations.

Figure 2 shows the orbital period and radius of the largest transiting planet belonging to each star. The left panel identifies the stars with reliable photometric periods. The right panel assigns colors to the data points based on categories that seem astrophysically distinct and that we chose to track separately throughout this study. Red is for hot Jupiters, defined by the criteria $R_{\rm p} > 7\ R_\oplus$ and $P_{\rm orb} < 13$ days. Green is for wider-orbiting giant planets, as well as planets within the "hot Neptune desert" identified by Mazeh et al. (2016). To qualify for this category, the planet radius must either exceed 5 $R_\oplus$ or the radius defined by the line connecting the points (2.5, 3) and (4, 10) in radius-period space. Blue is for the remaining planets, constituting the bulk of the sample.

3. PROJECTED AND TRUE ROTATION VELOCITIES

For each star with a reliably measured photometric period, we assumed that the photometric period is the stellar rotation period and computed $v \equiv 2\pi R_\star / P_{\rm rot}$. By using the same letter v that appears in $v \sin i$, we implicitly assumed they refer to the same rotation velocity, i.e., we neglected systematic errors due to differential rotation on both the measurement of $v \sin i$ from the spectral lines and on the determination of $P_{\rm rot}$ from the photometric variations. These are expected to be 5-10% effects (Hirano et al. 2014) and to at least partly cancel out; differential rotation causes both the inferred v and $v \sin i$ to be biased toward lower values than $v_{\rm eq}$ and $v_{\rm eq} \sin i$, where $v_{\rm eq}$ is the equatorial rotation velocity.

Figure 3 shows the results. The different panels use color to distinguish between different subsamples: by planet type (upper left), single vs. multiple transiting planets (upper right), and hot vs. cool stars (lower left). The lower right panel helps to put these results into perspective by showing synthetic $v \sin i$ data for an isotropically oriented population of stars. The synthetic data were generated by adopting the values of v from the data, drawing $\cos i$ from a uniform distribution, and multiplying v by $\sin i$.

For velocities below about 4 km s^{-1}, the large fractional uncertainties make it is difficult to make any useful comparisons. For higher velocities, the stars with reliable periods cluster around the identity line. The standard deviation of $v \sin i - v$ is 1.0 km s^{-1}, similar to the measurement uncertainty. This implies $\sin i \approx 1$. Since the orbital inclination also has $\sin i_{\rm o} \approx 1$, these results are consistent with (but do not require) a low obliquity.

We used these data to establish lower limits on the inclination of each star, focusing attention on the stars with $v > 4$ km s^{-1} for which meaningful constraints are possible. We chose to express the constraints as upper limits on $\cos i$. This facilitates the interpretation because $\cos i$ is uniformly distributed for a population of randomly oriented stars. Following Morton & Winn (2014)[3], the likelihood function is

$$\mathcal{L}(\text{data} \,|\, \cos i) = \int_0^\infty u p_1(u) p_2\left(\frac{u}{\sqrt{1-\cos^2 i}}\right) du, \quad (4)$$

[3] We note that Equation (13) of Morton & Winn (2014) has an error: it is missing the factor of u in the integral.

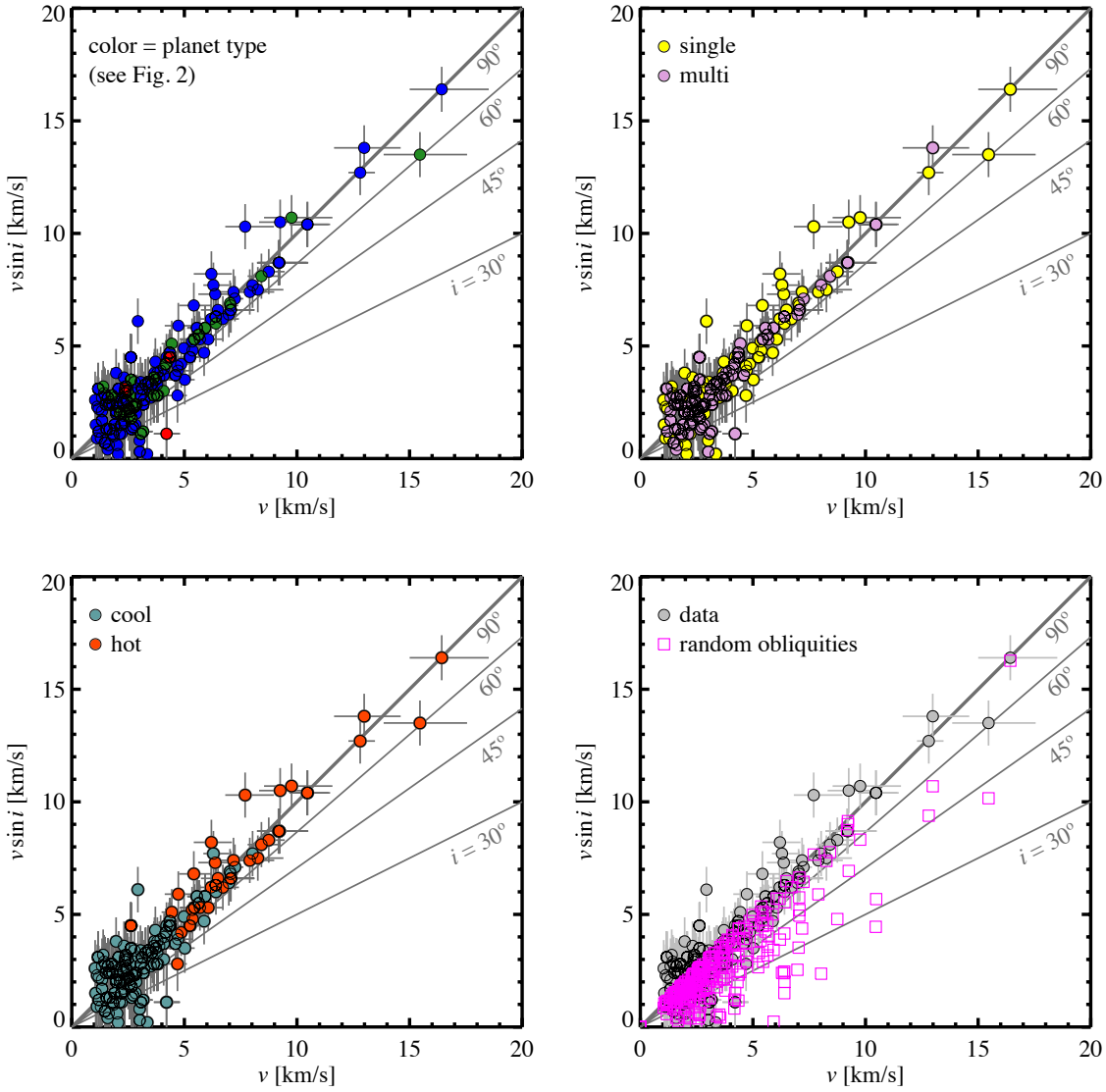

Figure 3. Measured sky-projected rotation velocity versus calculated true rotation velocity. Any points falling below the identity line are candidate misaligned stars ($\sin i < 1$). *Upper left.*—Color indicates planet type, using the same scheme as in Fig. 2. *Upper right.*—Color indicates whether the star has more than one detected transiting planet. *Lower left.*—Color indicates whether the star is hotter or cooler than 6000 K. *Lower right.*—Gray points are real data. The magenta squares are synthetic data with the same values of v as real data and values of $\sin i$ chosen from a distribution of random orientations.

where $p_1(u)$ and $p_2(u)$ are the likelihoods for v and $v \sin i$, respectively, based on the data. We assume p_1 and p_2 to be Gaussian functions with means and standard deviations set by the measured value and 1σ uncertainties.

Table 1 gives the results for each star. The 95% confidence upper limits on $\cos i$ range from 0.5 to 0.8 for most stars, with a mean of 0.7. Thus, one way to summarize this investigation is an unsuccessful search for any inclinations lower than about $\cos^{-1}(0.7)$ or 45°. These constraints are relatively weak, for reasons explained in the introduction. Even if a completely random orientation is chosen for a given star, there is a 70% chance that $\cos i$ will be smaller than 0.7.

We may draw stronger conclusions about the ensemble of stars. Visual inspection of the lower right panel of Figure 3 indicates that the data are incompatible with an isotropic distribution of obliquities: there are not enough low values of $v \sin i$. To quantify this impression, we compute the probability of drawing N stars from an isotropic distribution, each of which is observed to have $\cos i < z_i$:

$$p_{\rm iso} = \prod_{i=1}^{N} z_i. \quad (5)$$

For the 54 stars with $v > 4$ km s^{-1}, we find $p_{\rm iso} = 1.5 \times 10^{-9}$. For the subsample of 32 hot stars, a sample we will discuss further in § 6, we find $p_{\rm iso} = 2 \times 10^{-6}$.

We also constrained the obliquity distribution using a hierarchical Bayesian method, as advocated by Morton & Winn (2014). We assumed the obliquities follow a Rayleigh distribution,

$$p(\theta) = \frac{\theta}{\sigma^2} \exp(-\theta^2/2\sigma^2), \quad (6)$$

and used a Monte Carlo Markov Chain to determine the posterior distribution for σ, the mean obliquity. For each proposed value of σ, we drew N obliquities from the corresponding Rayleigh distribution, one for each star in the sample. We also drew N azimuthal angles ϕ from a uniform distribution and calculated $\sin i$ for each star using Eqn. 2. The likelihood function was taken to be proportional to $\exp(-\chi^2/2)$ with

$$\chi^2 = \sum_{i}^{N} \left[\frac{v \sin i - v \times \sin i}{\sqrt{\sigma^2_{v \sin i} + \sigma^2_v}} \right]^2. \quad (7)$$

Here, the sum is over all the stars in the sample: v and $v \sin i$ are the true and projected rotation rates, with uncertainties $\sigma_{v \sin i}$ and σ_v; and $\sin i$ is the value assigned through the Monte Carlo procedure described above. We adopted a uniform prior for σ.

For the sample of 58 stars with $v > 4$ km s^{-1}, we found $\sigma < 20°$ with 99% confidence. Broader distributions do not fit the data because they tend to produce too many low values of $\sin i$. Considering only the hot stars, cool stars, singles, and multis, the upper limits are 22°, 36°, 24° and 26°, respectively. We find no evidence for any distinction between these subsamples.

In interpreting these results we must remember that the stars are not a random selection of *Kepler* planet-hosting stars: they were selected by virtue of having a robustly detectable photometric period. Stars with low inclinations present lower-amplitude photometric signals associated with rotation. This should cause a sample of stars with detected signals to be deficient in low-inclination stars compared to the broader sample of stars with transiting planets. Suppose that the photometric variability amplitude varies as $\sin i$, and that a reduction in the amplitude by a factor f would have made it impossible to detect the rotation period. Then the revised probability that the stars belong to an isotropically oriented population is

$$p_{\rm iso} = \prod_{i=1}^{N} \frac{z_i}{\sqrt{1 - f_i^2}}. \quad (8)$$

The appropriate values of f_i would need to be determined by modeling the detection process for the rotation periods, which is beyond the scope of this study.

Hence, we are not yet in a position to use these data to draw firm conclusions about the obliquity distribution of planet-hosting stars in general. Despite this caveat, though, the conclusion that an isotropic distribution is ruled out seems secure. We find $p_{\rm iso} < 0.01$ even for $f = 2/3$, i.e., the case in which the photometric signals would have been undetectable had the amplitudes been lower by only 33%.

4. STARS WITH ANOMALOUSLY LOW $V \sin I$

Main-sequence stars of a given mass and age tend to have similar rotation velocities. This fact is the basis of gyrochronology, the determination of a star's age from its observed rotation velocity (Barnes 2003). It is also the basis of a method for identifying stars being viewed at low inclination: such stars should have an unusually low sky-projected rotation velocity. Figure 4 shows the CKS measurements of $v \sin i$ as a function of effective temperature, for all stars deemed "dwarfs" according to the boundary line shown in Figure 1. The points are color-coded to convey the type of planet, and also whether the star has more than one detected planet.

The rise in velocities with effective temperature, starting at around 6000 K, is a manifestation of the Kraft break.[4] Cooler stars have thick convective envelopes and develop strong magnetic activity, allowing them to lose angular momentum through magnetized winds. Hotter stars lack this spin-down mechanism and retain their initially rapid rotation rates. For stars cooler than the Kraft break, the typical rotation velocity is only a few km s^{-1}, which is not much larger than the measurement unceratinty. This makes it impossible to identify cases of unusually low $v \sin i$. More useful for this technique are the stars hotter than 6000 K. We searched this sample of 159 hot stars for unusually low $v \sin i$ values in two ways.

The first method was to identify the largest outliers from the overall trend of rising $v \sin i$ with effective temperature.

[4] The slight decrease in velocity between 4600 and 5200 K is harder to understand. To our knowledge this has not been observed before, and there is no evidence for such a trend in the large catalog of *Kepler* rotation periods (McQuillan et al. 2014). Possibly, it is an artifact of adopting the simple relationship of Valenti & Fischer (2005) between rotation and macroturbulence. These coolest stars play little to no role in our analyses.

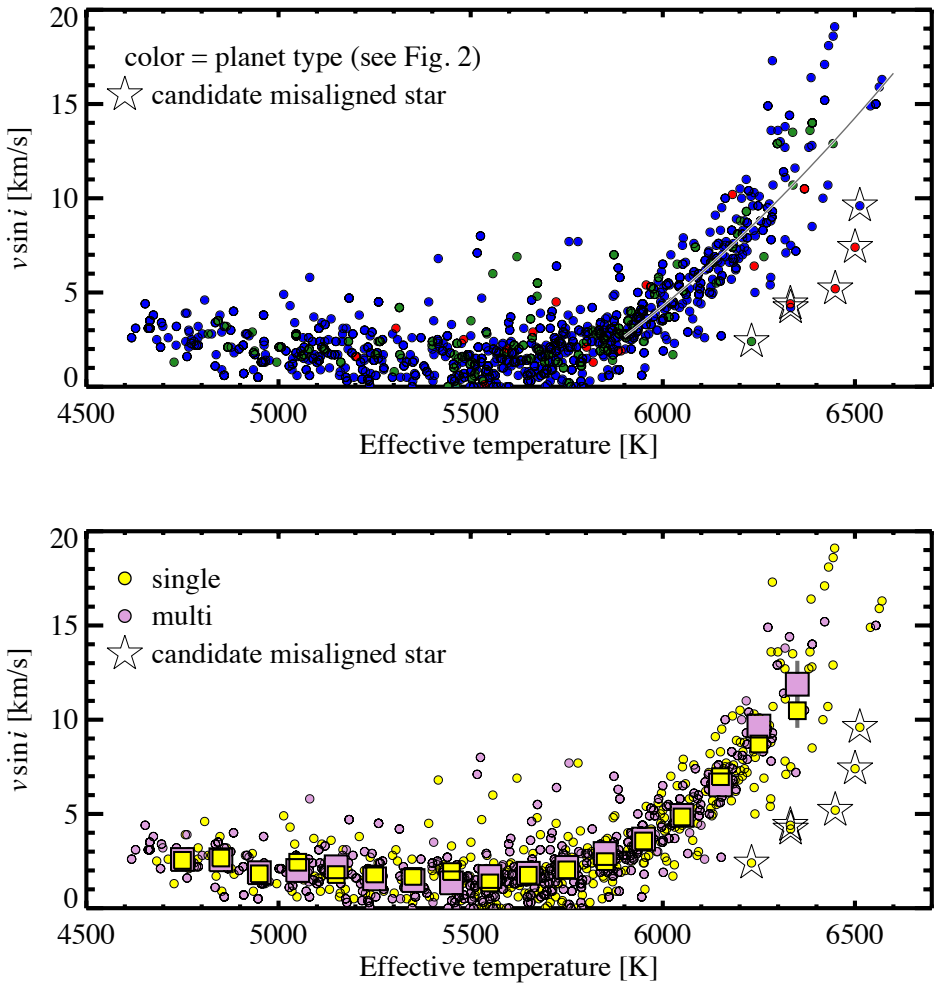

Figure 4. Projected rotation velocities as a function of effective temperature. *Top.*—Color coded according to planet type, using the same categories as in Fig. 2. The gray line is a fit to the data with $T_{\rm eff} > 5900$ K. The starred points are the most negative outliers from the fit, making them candidate misaligned stars. *Bottom.*—Color coded to distinguish singles and multis. The large squares show the averages within 100 K temperature bins.

We fitted the $v \sin i$ data with a quadratic function of $T_{\rm eff}$, and computed the normalized residual,

$$\Delta \equiv \frac{(v \sin i)_{\rm fit} - (v \sin i)_{\rm obs}}{\sigma_v} \quad (9)$$

for each star. Then we identified the systems with the largest values of Δ. There are six outliers with $\Delta > 5$, identified by the starred points in Figures 4 and 5. All six of these stars have only one detected transiting planet. Three of them are hot-Jupiter hosts: KOI 2 (HAT-P-7 or Kepler-2), KOI 18 (Kepler-5), and KOI 98 (Kepler-14). This is remarkable because there are only five hot-Jupiter hosts in the entire sample. If we were to select six stars randomly from the sample of 159 hot stars, the chance of selecting at least three hot-Jupiter hosts is 6×10^{-4}. This suggests that among the hot stars, those with hot Jupiters are more likely to have high obliquities than those without hot Jupiters.

The obliquity of HAT-P-7 was already known to be large, thanks to observations of the Rossiter-McLaughlin effect (Narita et al. 2009; Winn et al. 2009a) and rotational splittings of asteroseismic p-mode frequencies (Benomar et al. 2014; Lund et al. 2014). HAT-P-7 and Kepler-5 were also flagged by Schlaufman (2010) as likely misaligned, based on their low values of $v \sin i$. We are not aware of any direct determinations of the obliquity of Kepler-14.

The other three stars with anomalously low $v \sin i$ are KOI 167 (Kepler-480), KOI 1117 (Kepler-774), and KOI 1852 (Kepler-982), which host planets of size 2–3 $R_\oplus$ and orbital periods of 5–15 days. These are good candidates for follow-up observations to test for a high obliquity.

Our second method for identifying stars with anomalously low $v \sin i$ was to compute the rotation statistic Θ devised by Schlaufman (2010), which compares the observed $v \sin i$ to the expected rotation velocity v for the given type of star. The inputs were the star's $v \sin i$ from Petigura et al. (2017), and the stellar mass and age estimated by Johnson et al. (2017) by fitting stellar-evolutionary models to the observed spectroscopic parameters. The output, shown in Figure 5, is roughly the number of sigma by which $v \sin i$ is lower than expected. Schlaufman (2010) calibrated the statistic by applying it to

the sample of Valenti & Fischer (2005), finding that stars with $\Theta \gtrsim 2.9$ are likely to be misaligned. By this criterion the following systems are flagged as misaligned: KOI 2 (HAT-P-7), KOI 18 (Kepler-5), and KOI 2904 (Kepler-1382).

The first two members in this list were also flagged by the Δ statistic. The last member, KOI 2904, has $v \sin i = 7.5$ km s^{-1} and $T_{\rm eff} = 6139$ K. It does not stand out in Figure 4. It is nevertheless assigned a large Θ of 3.3 because the spin-down model of Schlaufman (2010) predicts a rotation period of 4.3 days, which, when combined with the stellar radius of 1.94 $R_\odot$ leads to an expected $v = 24$ km s^{-1}. This prediction is probably faulty, though. Although the star is classified as a "dwarf" according to the simple boundary drawn in Figure 1, the stellar-evolutionary modeling of Johnson et al. (2017) suggests it has begun evolving into a subgiant, and has likely slowed its rotation as it has expanded. This type of evolution is not taken into account in the spin-down model. Work is underway by K. Schlaufman on a revised statistic in which the model for rotational evolution can accommodate somewhat evolved stars.

5. COMPARING $V \sin I$ DISTRIBUTIONS

We also sought evidence for differences in the $v \sin i$ distributions between groups of stars. Any such differences might be attributed to differences in obliquity. An ideal basis for comparison would be a large sample of $v \sin i$ measurements of stars spanning the same range of spectroscopic parameters as the CKS stars that could be safely assumed to be randomly oriented and to share the same distribution of rotation velocities as the planet hosts. One could use the $v \sin i$ distribution of this control sample to determine the intrinsic rotation velocity distribution of the relevant population of stars (Chandrasekhar & Münch 1950). This could then be compared to the $v \sin i$ distribution of the hosts of transiting planets, to learn about the distribution of $\sin i$.

An attractive possibility is the sample of stars analyzed by Valenti & Fischer (2005) and Brewer et al. (2016), in the program entitled Spectral Properties of Cool Stars (SPOCS). The SPOCS stars were chosen to be targets for a Doppler exoplanet survey, and have been observed with the same instrument (Keck/HIRES) as the CKS stars. In almost all cases the choice to perform high-resolution spectroscopy was made without any prior knowledge of exoplanets, transiting or otherwise. Thus, it would seem that the spatial orientation of the stars should be random, as desired. A problem, though, is that the surveyors excluded stars for which the available information indicated possible problems with precise Doppler observations. They avoided close binaries. They also rejected young and chromospherically active stars based on published activity indicators (S and $R'_{\rm HK}$), X-ray fluxes, cluster-based ages, and lithium abundances. The resulting sample is therefore biased to some degree against rapid rotators, calling into question the assumption that the control stars and and planet-hosting stars have the same intrinsic distribution of rotation velocities.

Despite this flaw, we decided to try this comparison because the SPOCS stars come closer to the ideal than any other sample we were able to find. For consistency, we redetermined the $v \sin i$ values of the SPOCS stars using the same version of the SpecMatch software that was used on the CKS spectra. Figure 6 compares the projected rotation velocities of the planet-hosting stars (CKS) and control stars (SPOCS). Shown are the data for individual stars, as well as the averages within 100 K temperature bins. We excluded the hot-Jupiter hosts from the averages because such stars are already known to have a broad range of obliquities, and we wanted to probe the obliquities of hot stars with other types of planets. Assuming (i) the CKS and SPOCS stars have identical distributions of rotation velocities, (ii) the CKS stars have low obliquities, and (iii) the SPOCS stars are randomly oriented, we should observe that the mean $v \sin i$ of the SPOCS stars is lower than that of the CKS stars by a factor of $\pi/4$.

The data are compatible with these assumptions. The solid line in Figure 6 is a quadratic fit to the CKS data, providing an estimate of the mean $v \sin i$ as a function of effective temperature. The dashed line is the same function after multiplication by $\pi/4$, which gives a reasonable fit to the SPOCS data. In particular, the ratios of mean $v \sin i$ in the hottest two temperature bins are 0.759 ± 0.059 and 0.861 ± 0.091, which are both consistent with $\pi/4 \approx 0.785$. Thus, despite well-founded concerns about the control sample, there is suggestive evidence that hot stars lacking hot Jupiters have low obliquties.

Independently of the control sample, we searched for differences between the $v \sin i$ distributions of different subsamples of the planet-hosting stars. Since it has been suggested that the multis have systematically lower obliquities than the singles (Morton & Winn 2014), we binned the $v \sin i$ data in temperature for these two populations separately. These binned results for the singles and multis are shown with large squares in the bottom panel of Figure 4. There are no statistically significant differences, except for perhaps the two hottest temperature bins (>6200 K), within which the mean $v \sin i$ of the multis is higher than that of the singles by 0.9 and 0.5σ. Thus, this test revealed no compelling difference between singles and multis.

We also tried comparing the distributions of the Δ and Θ statistics described in the previous section. Both of these statistics are meant to quantify the difference between the observed $v \sin i$ and the rotation velocity one would expect for a star of the given type. Two-sided Kolmogorov-Smirnoff tests do not reveal any significant differences between multis and singles ($p = 0.4$ and 0.6 for Δ and Θ, respectively). Likewise, there do not appear to be any discernible differences between hosts of different planet types, apart from hot Jupiters.

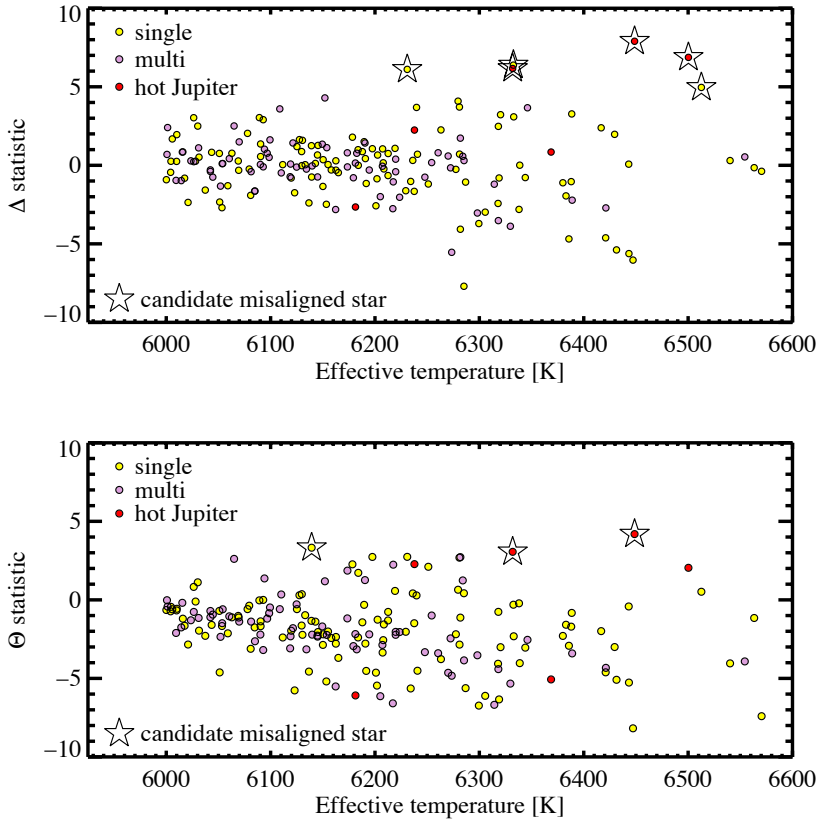

Figure 5. Rotation statistics. *Top.*—Deviation Δ from the best-fitting quadratic function of $v \sin i$ versus effective temperature. Large Δ implies an anomalously slow $v \sin i$. The starred points are the same as those in Fig. 2. *Bottom.*—The Schlaufman (2010) Θ statistic, which is high when the star appears to be rotating anomalously slowly. The starred points are those with Θ above the threshold of 2.9.

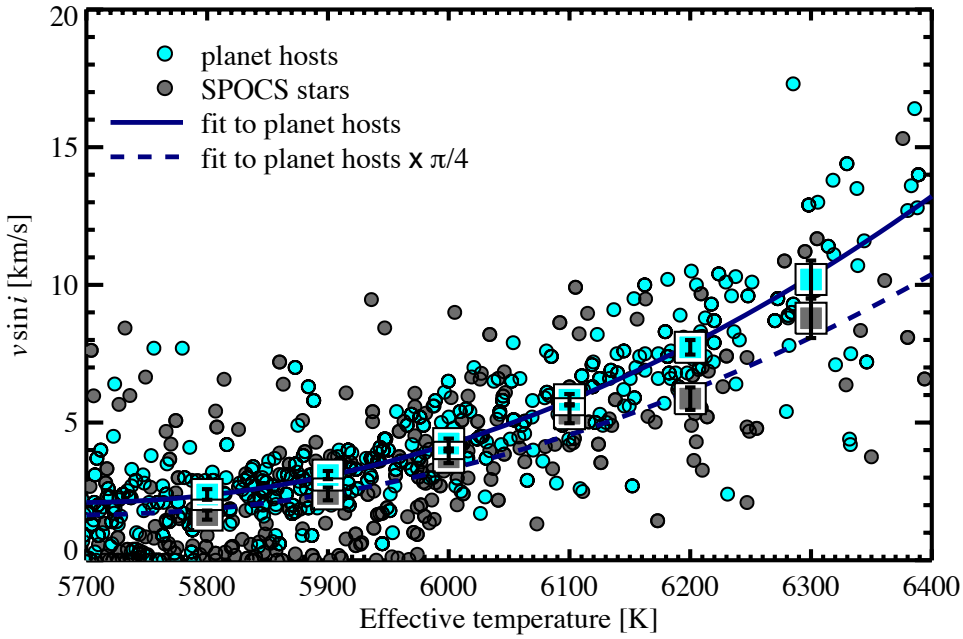

Figure 6. Comparison with a control sample of stars from the SPOCS catalog, assumed to be randomly oriented. The squares are averages within 100 K temperature bins. At a given effective temperature, the mean $v \sin i$ of the control stars appears to be lower than that of the planet-hosting stars by a factor of approximately $\pi/4$. This suggests that the planet hosts have low obliquites.

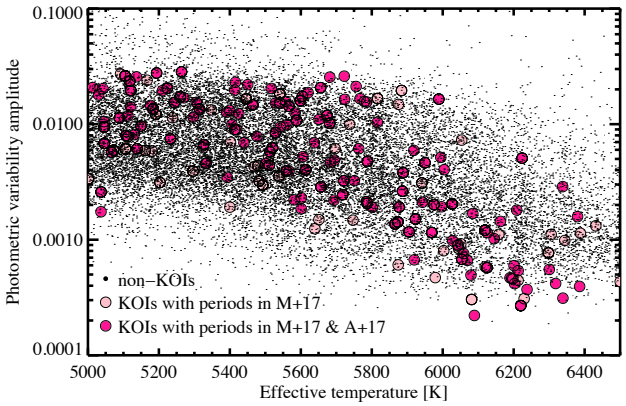

Figure 7. Photometric variability amplitudes. The small points are for stars without any detected transiting planets. The open circles are stars with transiting planets for which Mazeh et al. (2015) detected the rotation period, and the solid red symbols are stars for which Angus et al. (2017) agree on the period. This subset, analyzed in § 3, does not appear to be biased toward higher variability (higher $\sin i$) than the other planet-hosting stars in the same temperature range.

6. SUMMARY AND DISCUSSION

Using the newly available CKS data, we have investigated the obliquity distribution of *Kepler* stars by comparing measurements of v and $v \sin i$, seeking evidence for anomalously low $v \sin i$ values, and testing for systematic differences between the $v \sin i$ distributions of different groups of stars.

Among the stars with reliably measured photometric periods, we found no evidence for high obliquities. When modeled as a Rayleigh distribution, the mean obliquity is smaller than 20° with 99% confidence. An isotropic distribution is strongly ruled out, both for the entire sample, and for the subset of hot stars ($T_{\rm eff} > 6000$ K). One reason this is interesting is that hot stars with hot Jupiters are known from prior observations to have a very broad obliquity distribution. Not as much was known about hot stars without hot Jupiters; our findings suggest they tend to have lower obliquities.

Walkowicz & Basri (2013) and Hirano et al. (2014) also sought possible cases of spin-orbit misalignment through discrepancies between $v \sin i$ and v, based on the data available at the time. Table 2 summarizes our results for the objects that they highlighted as possibly misaligned. The column labeled N_σ is the number-of-sigma by which v exceeds $v \sin i$, which is smaller than 2 in all cases. Thus, we do not find compelling evidence for misalignments in these systems based on the CKS data, although it still may be worth follow-up observations to determine the obliquities with other techniques.

We can also compare our results directly to the study of Mazeh et al. (2015). As mentioned in § 1 their insight was to compare the photometric variability amplitudes of the stars with transiting planets (KOIs) and the much larger sample of stars without known transiting planets (non-KOIs). Figure 7 reproduces this comparison over the temperature range 5000-6500 K. Among the cool stars, the KOIs show stronger variability than the non-KOIs. More puzzling is that for hot stars, the KOIs are *less* variable than the non-KOIs. An interpretation purely in terms of obliquities is problematic. If photometric variability scales with $\sin i$, one would think that the obliquity distribution producing the lowest level of variability would be an isotropic distribution. Even lower variability would require preferential alignment of stellar rotation axes with the line of sight, which seems implausible. How, then, could the KOIs have a lower level of variability than the non-KOIs, which presumably have an isotropic distribution?

At least part of the explanation is a selection effect: the sample of stars with detected transiting planets is biased toward lower variability because it is more difficult to detect planets around highly variable stars. The bias should be most pronounced for hot stars because they are larger, causing the transit signals to be smaller and closer to the detection threshold. Mazeh et al. (2015) modeled the selection process and found that the level of bias could account for about half of the difference in the observed variability between KOIs and non-KOIs. This left open the possibility that the variability of hot KOIs and non-KOIs is indeed nearly the same, which would imply that hot stars have nearly random obliquities. This would be an important result because, as noted above, almost all the prior work was restricted to stars with hot Jupiters. If the high obliquities are a more general phenomenon, this would point toward theories involving mainly the star, rather than the disk, planetary dynamics, or spin-orbit resonances.

However, our investigation of these stars (§ 3) is not compatible with this interpretation of the variability data. The sample contains 30 hot stars with reliably measured photometric periods that are all compatible with high inclination and low obliquity; they cannot be drawn from an isotropic distribution. While it is true that these 30 stars are only a subset of those examined by Mazeh et al. (2015), there does not appear to be any reason for them to be relatively biased toward high inclination. Figure 7 shows that they have the same mean variability level as the larger sample.

We placed an upper limit on the fraction of the hot stars in our sample that could have been drawn from an isotropic distribution in the following manner:

1. Randomly select a subset n of the hot stars.
2. Calculate $p_{\rm iso}$ based only on these n stars.
3. Repeat the preceding steps 100 times to obtain the mean value of $p_{\rm iso}$ for that choice of n.
4. Repeat the preceding steps for all n ranging from 1 to 30, and find $n_{\rm max}$ for which $p_{\rm iso} < 0.01$.

The result is $n_{\rm max} = 11$ out of 33, i.e., fewer than one-third of the hot stars are drawn from a randomly oriented distribution. Given this result, we consider the interpretation of the variability-amplitude data for hot stars to remain murky.

In the second part of the study, we identified some individual stars that have unusually low projected rotation rates: KOI 2 (HAT-P-7), KOI 18 (Kepler-5), KOI 98 (Kepler-14), KOI 167 (Kepler-480), KOI 1117 (Kepler-774), and KOI 1852 (Kepler-982). These are good candidates for high-obliquity stars. Three of these are hot-Jupiter hosts and indeed one of them (HAT-P-7) was already known to have a high obliquity. These results support the notion that high

obliquities are more common among stars with hot Jupiters, compared to those hosting other types of planets. We also compared the $v \sin i$ distributions between different samples of KOIs using several statistics, and found no significant differences.

In neither part of our study did we find evidence that the multis have lower obliquities than the singles, a trend that had been noted by (Morton & Winn 2014). Our non-confirmation of this result leads us to suspect the result was spurious. The trend was seen with only 2σ confidence, and was based on a study of a smaller number of stars (75) and a more heterogeneous dataset (drawn from 5 different sources).

An important lesson we drew from this study is that hot stars lacking hot Jupiters generally seem to have low obliquities. This is the converse of what was already known: hot stars with hot Jupiters tend to have high obliquities (Winn et al. 2010a; Albrecht et al. 2012). Together these findings suggest that the high obliquities are related to the presence of close-in giant planets: the planet is somehow to blame for the misalignment, or is at least associated with the causes of misalignment. This argues against theories in which high obliquities are a consequence of star-disk misalignment (Batygin 2012) or of processes taking place wholly within the star (Rogers et al. 2012). Instead, this result points toward a theory that requires a close-in giant planet, while also making a distinction between hot stars and cool stars.

In the theory of Spalding & Batygin (2015), spin-orbit misalignments erupt from a resonance between the precession of the stellar spin axis induced by a protoplanetary disk, and the precession of the disk induced by a distant stellar companion. Cool stars are able to realign with their disks through magnetic torques, but hot stars cannot because of their weaker and more disorderly magnetic fields. In this scenario, hot stars should be misaligned with the orbits of all the planets that ultimately form within the disk, and not just hot Jupiters. This does not seem compatible with our results. In addition this mechanism cannot explain those few cool stars that are known to have high obliquities, such as HD 80606 (Winn et al. 2009b; Hébrard et al. 2010), WASP-8 (Queloz et al. 2010), and HAT-P-11 (Winn et al. 2010b; Hirano et al. 2011). One would need to invoke a separate mechanism for such cases, such as Kozai-Lidov oscillations (Fabrycky & Tremaine 2007).

Matsakos & Königl (2015) proposed an interesting alternative: (i) stars generally become misaligned with their disks (and hence the planetary orbits) due to torques from nearby stars; (ii) many stars also ingest a hot Jupiter early in their lifetimes, causing them to realign with the planetary orbital plane; and (iii) this realignment cannot be achieved for hot stars because of their higher mass and angular momentum. This theory, as desired, distinguishes between hot and cool stars and requires a close-in giant planet. However, in this story the guilty planet no longer exists. Our findings suggest that the high obliquities are characterstic of stars with a currently existing hot Jupiter.

Even after the infusion of new data from the California-*Kepler* Survey, we have only limited information about the obliquities of the *Kepler* planet-hosting stars. As we emphasized in § 3, our ability to draw general conclusions would be enhanced by a reliable quantitative model for the selection function associated with the detection of the photometric rotation period. The current sample is biased toward low obliquity to some degree, because of the requirement that the photometric variations must be robustly detected.

Another path forward would be to improve upon the existing control sample of stars. Ideally, we would measure the $v \sin i$ distribution of a sample of at least several hundred *Kepler* stars selected without regard to rotation velocity, orientation, or planet detection, spanning the same range of spectroscopic parameters as the planet hosts. The SPOCS sample that we employed in § 5 was not designed for this purpose. It is smaller than the sample of planet-hosting stars, and relatively deficient in hot stars. Furthermore, at a given effective temperature it is probably biased against rapid rotators due to a selection against young and chromospherically active stars.

Finally, it is still valuable to perform Rossiter-McLaughlin observations, analyze spot-crossing events, and perform other tests of obliquities in individual systems. This remains difficult for the relatively faint *Kepler* stars, but will be much easier with stars that are 2-3 mag brighter, as we hope will be found by NASA's forthcoming *Transiting Exoplanet Survey Satellite* (Ricker et al. 2015).

We are grateful to the other CKS team members, and the NASA *Kepler* team, for producing the database upon which this study is based. E.A.P. acknowledges support from Hubble Fellowship grant HST-HF2-51365.001-A awarded by the Space Telescope Science Institute, which is operated by the Association of Universities for Research in Astronomy, Inc. for NASA under contract NAS 5-26555. S.A. and A.B.J. acknowledge support from the Danish Council for Independent Research, through a DFF Sapere Aude Starting Grant nr. 4181-00487B. The authors also wish to recognize and acknowledge the very significant cultural role and reverence that the summit of Maunakea has always had within the indigenous Hawaiian community. We are most fortunate to have the opportunity to conduct observations from this mountain.

REFERENCES

Albrecht, S., Winn, J. N., Marcy, G. W., et al. 2013, ApJ, 771, 11
Albrecht, S., Winn, J. N., Johnson, J. A., et al. 2012, ApJ, 757, 18
Angus, R., Morton, T., Aigrain, S., Foreman-Mackey, D., & Rajpaul, V. 2017, ArXiv e-prints, arXiv:1706.05459 [astro-ph.SR]
Barnes, S. A. 2003, ApJ, 586, 464
Batalha, N. M., Borucki, W. J., Koch, D. G., et al. 2010, ApJL, 713, L109
Batygin, K. 2012, Nature, 491, 418
Benomar, O., Masuda, K., Shibahashi, H., & Suto, Y. 2014, PASJ, 66, 94
Brewer, J. M., Fischer, D. A., Valenti, J. A., & Piskunov, N. 2016, ApJS, 225, 32
Campante, T. L., Lund, M. N., Kuszlewicz, J. S., et al. 2016, ApJ, 819, 85
Chandrasekhar, S., & Münch, G. 1950, ApJ, 111, 142

Chaplin, W. J., Sanchis-Ojeda, R., Campante, T. L., et al. 2013, ApJ, 766, 101
Chatterjee, S., Ford, E. B., Matsumura, S., & Rasio, F. A. 2008, ApJ, 686, 580
Coelho, P., Barbuy, B., Meléndez, J., Schiavon, R. P., & Castilho, B. V. 2005, A&A, 443, 735
Dawson, R. I. 2014, ApJL, 790, L31
Fabrycky, D., & Tremaine, S. 2007, ApJ, 669, 1298
Furlan, E., Ciardi, D. R., Everett, M. E., et al. 2017, AJ, 153, 71
Gratia, P., & Fabrycky, D. 2017, MNRAS, 464, 1709
Hébrard, G., Désert, J.-M., Díaz, R. F., et al. 2010, A&A, 516, A95
Hirano, T., Narita, N., Shporer, A., et al. 2011, PASJ, 63, 531
Hirano, T., Sanchis-Ojeda, R., Takeda, Y., et al. 2012a, ApJ, 756, 66
—. 2014, ApJ, 783, 9
Hirano, T., Narita, N., Sato, B., et al. 2012b, ApJL, 759, L36
Howard, A. W., Marcy, G. W., Bryson, S. T., et al. 2012, ApJS, 201, 15
Huber, D., Carter, J. A., Barbieri, M., et al. 2013, Science, 342, 331
Johnson, J. A., Petigura, E. A., Fulton, B. J., et al. 2017, ArXiv e-prints, arXiv:1703.10402 [astro-ph.EP]
Kraft, R. P. 1967, ApJ, 150, 551
Lund, M. N., Lundkvist, M., Silva Aguirre, V., et al. 2014, A&A, 570, A54
Matsakos, T., & Königl, A. 2015, ApJL, 809, L20
Mazeh, T., Holczer, T., & Faigler, S. 2016, A&A, 589, A75
Mazeh, T., Perets, H. B., McQuillan, A., & Goldstein, E. S. 2015, ApJ, 801, 3
McQuillan, A., Mazeh, T., & Aigrain, S. 2014, ApJS, 211, 24
Morton, T. D., Bryson, S. T., Coughlin, J. L., et al. 2016, ApJ, 822, 86
Morton, T. D., & Winn, J. N. 2014, ApJ, 796, 47
Mullally, F., Coughlin, J. L., Thompson, S. E., et al. 2016, PASP, 128, 074502
Narita, N., Sato, B., Hirano, T., & Tamura, M. 2009, PASJ, 61, L35
Otor, O. J., Montet, B. T., Johnson, J. A., et al. 2016, AJ, 152, 165
Petigura, E. A. 2015, PhD thesis, University of California, Berkeley
Petigura, E. A., Howard, A. W., Marcy, G. W., et al. 2017, ArXiv e-prints, arXiv:1703.10400 [astro-ph.EP]
Queloz, D., Anderson, D. R., Collier Cameron, A., et al. 2010, A&A, 517, L1
Ricker, G. R., Winn, J. N., Vanderspek, R., et al. 2015, Journal of Astronomical Telescopes, Instruments, and Systems, 1, 014003
Rogers, T. M., Lin, D. N. C., & Lau, H. H. B. 2012, ApJL, 758, L6
Sanchis-Ojeda, R., Fabrycky, D. C., Winn, J. N., et al. 2012, Nature, 487, 449
Sanchis-Ojeda, R., Winn, J. N., Marcy, G. W., et al. 2013, ApJ, 775, 54
Schatzman, E. 1962, Annales d'Astrophysique, 25, 18
Schlaufman, K. C. 2010, ApJ, 719, 602
Spalding, C., & Batygin, K. 2014, ApJ, 790, 42
—. 2015, ApJ, 811, 82
Struve, O. 1930, ApJ, 72
Triaud, A. H. M. J., Collier Cameron, A., Queloz, D., et al. 2010, A&A, 524, A25
Valenti, J. A., & Fischer, D. A. 2005, ApJS, 159, 141
Walkowicz, L. M., & Basri, G. S. 2013, MNRAS, 436, 1883
Winn, J. N., Fabrycky, D., Albrecht, S., & Johnson, J. A. 2010a, ApJL, 718, L145
Winn, J. N., & Fabrycky, D. C. 2015, ARA&A, 53, 409
Winn, J. N., Johnson, J. A., Albrecht, S., et al. 2009a, ApJL, 703, L99
Winn, J. N., Howard, A. W., Johnson, J. A., et al. 2009b, ApJ, 703, 2091
Winn, J. N., Johnson, J. A., Howard, A. W., et al. 2010b, ApJL, 723, L223

Table 1. Stars with reliable rotation periods

KOI number	KIC number	$T_{\rm eff}$ [K]	$\log g$ [cgs]	Radius [$R_\odot$]	Rotation Period [days]	v [km s^{-1}]	$v \sin i$ [km s^{-1}]	$\cos i_{\rm max}$ (95% conf.)
49	9527334	5779 ± 70	4.338 ± 0.10	$1.08^{+0.14}_{-0.09}$	8.665 ± 0.075	6.421 ± 0.62	7.70 ± 1.00	0.54
85	5866724	6219 ± 70	4.213 ± 0.10	$1.43^{+0.23}_{-0.17}$	7.889 ± 0.210	9.313 ± 1.14	8.70 ± 1.00	0.67
107	11250587	5919 ± 70	4.098 ± 0.10	$1.62^{+0.29}_{-0.22}$	17.499 ± 0.800	4.747 ± 0.56	3.90 ± 1.06	0.83
203	10619192	5722 ± 70	4.534 ± 0.10	$1.03^{+0.08}_{-0.05}$	12.161 ± 0.111	4.367 ± 0.26	4.50 ± 1.04	0.73
257	5514383	6162 ± 70	4.302 ± 0.10	$1.29^{+0.18}_{-0.13}$	7.900 ± 0.081	8.400 ± 0.94	7.50 ± 1.01	0.70
271	9451706	6124 ± 70	4.217 ± 0.10	$1.41^{+0.24}_{-0.16}$	10.151 ± 0.220	7.206 ± 0.87	6.60 ± 1.01	0.71
318	8156120	6338 ± 70	4.169 ± 0.10	$1.56^{+0.25}_{-0.19}$	5.117 ± 0.127	15.665 ± 1.85	13.50 ± 1.00	0.69
323	9139084	5528 ± 70	4.720 ± 0.10	$0.89^{+0.04}_{-0.03}$	7.621 ± 0.023	5.905 ± 0.22	4.70 ± 1.03	0.80
333	10337258	6208 ± 70	4.418 ± 0.10	$1.19^{+0.12}_{-0.08}$	6.909 ± 0.150	8.864 ± 0.60	8.30 ± 1.00	0.63
372	6471021	5815 ± 70	4.597 ± 0.10	$0.96^{+0.06}_{-0.04}$	11.887 ± 0.087	4.115 ± 0.20	3.00 ± 1.16	0.89
590	9782691	5975 ± 70	4.415 ± 0.10	$1.08^{+0.11}_{-0.08}$	13.482 ± 0.380	4.120 ± 0.27	3.70 ± 1.08	0.81
620	11773022	5673 ± 70	4.697 ± 0.10	$0.92^{+0.05}_{-0.03}$	8.212 ± 0.042	5.680 ± 0.23	5.50 ± 1.02	0.69
665	6685609	5969 ± 70	4.092 ± 0.10	$1.69^{+0.28}_{-0.26}$	15.703 ± 0.960	5.451 ± 0.65	5.30 ± 1.02	0.72
673	7124613	6380 ± 70	4.466 ± 0.10	$1.22^{+0.10}_{-0.06}$	4.842 ± 0.200	12.889 ± 0.59	12.70 ± 1.00	0.51
720	9963524	5260 ± 70	4.677 ± 0.10	$0.82^{+0.04}_{-0.03}$	9.529 ± 0.099	4.399 ± 0.15	4.50 ± 1.04	0.73
723	10002866	5314 ± 70	4.555 ± 0.10	$0.91^{+0.07}_{-0.04}$	11.060 ± 0.047	4.216 ± 0.24	4.20 ± 1.05	0.75
896	7825899	4973 ± 70	3.945 ± 0.10	$2.09^{+0.31}_{-0.28}$	25.132 ± 0.202	4.215 ± 0.58	1.10 ± 1.92	0.97
975	3632418	6202 ± 70	4.079 ± 0.10	$1.58^{+0.22}_{-0.19}$	12.553 ± 0.170	6.388 ± 0.77	7.30 ± 1.01	0.58
1353	7303287	5989 ± 70	4.596 ± 0.10	$1.03^{+0.07}_{-0.05}$	8.789 ± 0.059	5.960 ± 0.29	5.80 ± 1.01	0.68
1445	11336883	6318 ± 70	4.255 ± 0.10	$1.38^{+0.20}_{-0.15}$	5.389 ± 0.102	13.209 ± 1.48	13.80 ± 1.00	0.53
1612	10963065	6089 ± 70	4.305 ± 0.10	$1.17^{+0.14}_{-0.11}$	12.650 ± 0.300	4.719 ± 0.42	2.80 ± 1.21	0.93
1616	9015738	6042 ± 70	4.265 ± 0.10	$1.30^{+0.19}_{-0.14}$	11.711 ± 1.550	5.763 ± 0.61	5.30 ± 1.02	0.74
1621	5561278	6079 ± 70	4.038 ± 0.10	$1.68^{+0.26}_{-0.22}$	17.975 ± 0.420	4.758 ± 0.57	5.90 ± 1.01	0.61
1628	6975129	6223 ± 70	4.484 ± 0.10	$1.17^{+0.10}_{-0.06}$	5.731 ± 0.650	10.561 ± 0.86	10.40 ± 1.00	0.57
1800	11017901	5620 ± 70	4.686 ± 0.10	$0.91^{+0.05}_{-0.03}$	6.536 ± 0.046	7.068 ± 0.27	6.90 ± 1.01	0.63
1825	5375194	5390 ± 70	4.687 ± 0.10	$0.86^{+0.04}_{-0.03}$	10.337 ± 0.194	4.231 ± 0.13	4.50 ± 1.04	0.72
1839	5856571	5517 ± 70	4.665 ± 0.10	$0.90^{+0.05}_{-0.03}$	6.280 ± 0.020	7.309 ± 0.33	7.10 ± 1.01	0.63

Table 1 continued

Table 1 *(continued)*

KOI number	KIC number	$T_{\rm eff}$ [K]	$\log g$ [cgs]	Radius [$R_\odot$]	Rotation Period [days]	v [km s^{-1}]	$v \sin i$ [km s^{-1}]	$\cos i_{\rm max}$ (95% conf.)
1883	11758544	6059 ± 70	4.148 ± 0.10	$1.49^{+0.23}_{-0.19}$	11.632 ± 0.280	6.495 ± 0.76	6.60 ± 1.01	0.66
1886	9549648	6200 ± 70	4.195 ± 0.10	$1.44^{+0.22}_{-0.18}$	7.641 ± 0.499	9.354 ± 0.94	10.50 ± 1.00	0.50
1958	9836149	5785 ± 70	4.575 ± 0.10	$0.97^{+0.07}_{-0.05}$	10.501 ± 0.111	4.741 ± 0.25	4.10 ± 1.05	0.80
2002	10024701	6004 ± 70	4.499 ± 0.10	$1.06^{+0.09}_{-0.06}$	10.083 ± 0.610	5.400 ± 0.31	4.80 ± 1.03	0.76
2026	11923284	5994 ± 70	4.516 ± 0.10	$1.01^{+0.08}_{-0.06}$	9.775 ± 0.120	5.320 ± 0.31	4.50 ± 1.04	0.79
2035	9790806	5557 ± 70	4.670 ± 0.10	$0.90^{+0.05}_{-0.03}$	7.113 ± 0.053	6.453 ± 0.28	6.00 ± 1.01	0.69
2109	11499228	6084 ± 70	4.093 ± 0.10	$1.59^{+0.26}_{-0.20}$	11.197 ± 0.090	7.324 ± 1.04	7.40 ± 1.01	0.66
2110	11460462	6385 ± 70	4.260 ± 0.10	$1.40^{+0.20}_{-0.13}$	4.326 ± 0.066	16.689 ± 1.80	16.40 ± 1.00	0.56
2111	8612275	5604 ± 70	4.589 ± 0.10	$0.93^{+0.06}_{-0.04}$	10.233 ± 0.054	4.656 ± 0.25	3.70 ± 1.08	0.84
2273	9717943	6028 ± 70	4.271 ± 0.10	$1.29^{+0.20}_{-0.13}$	12.507 ± 0.240	5.357 ± 0.59	4.50 ± 1.04	0.80
2403	2142522	6125 ± 70	4.323 ± 0.10	$1.25^{+0.15}_{-0.11}$	10.443 ± 0.130	6.156 ± 0.61	5.30 ± 1.02	0.76
2545	9696358	6197 ± 70	4.035 ± 0.10	$1.83^{+0.30}_{-0.26}$	17.069 ± 0.470	5.454 ± 0.71	6.80 ± 1.01	0.58
2555	5350244	6144 ± 70	4.349 ± 0.10	$1.18^{+0.14}_{-0.10}$	8.900 ± 0.110	6.844 ± 0.64	6.20 ± 1.01	0.71
2593	8212002	6212 ± 70	4.259 ± 0.10	$1.35^{+0.21}_{-0.14}$	8.690 ± 0.180	8.061 ± 0.93	7.40 ± 1.01	0.69
2632	11337566	6237 ± 70	4.059 ± 0.10	$1.68^{+0.30}_{-0.23}$	11.054 ± 0.210	7.856 ± 1.09	10.30 ± 1.00	0.47
2675	5794570	5755 ± 70	4.632 ± 0.10	$0.96^{+0.06}_{-0.04}$	6.071 ± 0.061	8.094 ± 0.37	7.70 ± 1.00	0.63
2678	6779260	5415 ± 70	4.703 ± 0.10	$0.86^{+0.05}_{-0.03}$	6.193 ± 0.017	7.099 ± 0.30	6.80 ± 1.01	0.65
2722	7673192	6119 ± 70	4.381 ± 0.10	$1.14^{+0.13}_{-0.09}$	9.069 ± 0.210	6.480 ± 0.48	6.30 ± 1.01	0.67
2961	10471515	6069 ± 70	4.311 ± 0.10	$1.25^{+0.17}_{-0.12}$	11.898 ± 0.440	5.394 ± 0.48	5.20 ± 1.02	0.72
3060	11019987	6189 ± 70	4.055 ± 0.10	$1.61^{+0.22}_{-0.19}$	13.174 ± 0.350	6.223 ± 0.67	6.20 ± 1.01	0.67
3681	2581316	6194 ± 70	4.292 ± 0.10	$1.29^{+0.19}_{-0.12}$	7.789 ± 0.475	8.455 ± 0.70	8.10 ± 1.00	0.63
3683	10795103	6338 ± 70	4.274 ± 0.10	$1.32^{+0.17}_{-0.12}$	6.899 ± 1.450	10.039 ± 1.49	10.70 ± 1.00	0.58
3835	2581554	5013 ± 70	4.703 ± 0.10	$0.78^{+0.03}_{-0.02}$	7.877 ± 0.029	5.006 ± 0.16	4.90 ± 1.03	0.71
4160	7610663	5766 ± 70	4.497 ± 0.10	$1.03^{+0.10}_{-0.06}$	10.418 ± 0.040	5.101 ± 0.37	3.50 ± 1.10	0.88
4246	5177859	5723 ± 70	4.624 ± 0.10	$0.99^{+0.06}_{-0.05}$	7.227 ± 0.057	7.018 ± 0.32	6.40 ± 1.01	0.69
4276	6026924	6300 ± 70	3.982 ± 0.10	$1.99^{+0.31}_{-0.28}$	16.212 ± 0.271	6.222 ± 0.87	8.20 ± 1.00	0.52
4411	5281113	6043 ± 70	4.348 ± 0.10	$1.12^{+0.13}_{-0.10}$	11.754 ± 1.390	4.896 ± 0.43	4.20 ± 1.05	0.80

Table 2. Stars previously identified as possibly misaligned

KOI number	KIC number	$T_{\rm eff}$ [K]	$\log g$ [cgs]	Radius [$R_\star$]	Rotation period[a] [days]	v [km s^{-1}]	$v \sin i$ [km s^{-1}]	N_σ[b]
261	5383248	5750 ± 70	4.504 ± 0.10	$0.99^{+0.08}_{-0.05}$	15.01 ± 0.10	3.34 ± 0.21	0.20 ± 2.00	1.57
323	9139084	5528 ± 70	4.720 ± 0.10	$0.89^{+0.04}_{-0.03}$	7.62 ± 0.00	5.87 ± 0.24	4.70 ± 1.03	1.11
377	3323887	5787 ± 70	4.473 ± 0.10	$1.02^{+0.10}_{-0.06}$	16.76 ± 0.09	3.07 ± 0.23	1.10 ± 1.92	1.02
988	2302548	5121 ± 70	4.687 ± 0.10	$0.81^{+0.04}_{-0.03}$	12.43 ± 0.01	3.28 ± 0.13	3.30 ± 1.12	–0.02
1890	7449136	6119 ± 70	4.190 ± 0.10	$1.43^{+0.24}_{-0.18}$	...	...	7.20 ± 1.01	...
2002	10024701	6004 ± 70	4.499 ± 0.10	$1.06^{+0.09}_{-0.06}$	10.08 ± 0.05	5.32 ± 0.36	4.80 ± 1.03	0.49
2026	11923284	5994 ± 70	4.516 ± 0.10	$1.01^{+0.08}_{-0.06}$	9.77 ± 0.05	5.25 ± 0.32	4.50 ± 1.04	0.70
2261	3734418	5176 ± 70	4.696 ± 0.10	$0.81^{+0.04}_{-0.03}$	11.43 ± 0.00	3.58 ± 0.14	3.10 ± 1.15	0.42

[a] A blank entry indicates that the photometric rotation period was not deemed to be reliable, i.e., the catalogs of Mazeh et al. (2015) and Angus et al. (2017) do not report consistent results.

[b] Defined as $v - v \sin i$ divided by the quadrature sum of the uncertainties in v and $v \sin i$.